Progress In Electromagnetics Research M, Vol. 104, 123–132, 2021

A Multi-Band Cylindrical Conformal Antenna with Low Specific Absorption Rate for Wireless Medical Capsule Endoscopy

Zhong Yu[1], Bingwen He[1, *], Xinguo Wu[1], and Xudong An[2]

Abstract—A multi-band cylindrical conformal endoscopy antenna with low specific absorption rate (SAR) is designed for endoscope applications, which covers the Industrial, Scientific and Medical bands (ISM 902–928 MHz, 2.4–2.4835 GHz), Medical Device Radio Communications Service band (MedRadio 401–406 MHz), and Wireless Medical Telemetry Service (WMTS 608–614 MHz). The proposed antenna radiates as a symmetrical meanderline structure with a center loaded parasitic opened-loop element, which is bent into the cylindrical conformal shape and wrapped onto the inner wall of the capsule shell. The parasitic opened-loop element excites low frequency resonance at 403 MHz and reduces the SAR values of the antenna. The measured relative bandwidth ($|S_{11}| < -10$ dB) of the antenna implements 133% ultra-wideband, ranging from 0.35 GHz to 1.76 GHz, and 39% wideband, ranging from 2.01 GHz to 3 GHz. The peak gains and the peak 1 g SAR values at 403 MHz, 611 MHz, 915 MHz, 2.4 GHz are -26.6 dBi, -18.9 dBi, -11.8 dBi, -11.3 dBi, and 83, 82, 94, 153 W/kg, respectively. The results indicate that the proposed antenna complies well with the human safety standards.

1. INTRODUCTION

The wireless medical capsule endoscopy (WMCE) is promising in medical domain owing to its more convenient technique than traditional endoscopy on gastrointestinal (GI) operation. WMCE provides accurate diagnostic information by establishing a communication link between the in-body device and outside equipment [1–3]. In WMCE systems, the antenna is one of the most pivotal components, which can ensure information transmission [4] rate in the link. The variable dielectric constants of human tissues cause the impedance mismatch of the antenna, which deteriorates the communication link. The multi-band can ensure the robustness of the communication link so that the antenna should cover MedRadio band (401–406 MHz), ISM bands (902–928 MHz, 2.4–2.4835 GHz), and WMTS band (608–614 MHz) [5]. Moreover, the low specific absorption rate (SAR) [6] guarantees users' safety, and the excellent low-frequency penetrativity satisfies the in-body and the outside communication of WMCE.

In [7, 8], two-layer or multi-layer structures are used to modify F structures for obtaining double-band or multi-band antennas of the MICS, ISM bands. Yousaf et al. proposed a multi-band meanderline conformal antenna integrated with a capsule system, covering the MedRadio, midfield, and ISM bands [9]. The low frequency bands of these antennas are narrow-band. Shang and Yu proposed a conformal Inverted-F (IFA) antenna by loading an L-shape open-slot on ground between the short point and feeding point to achieve a 100% ultrawideband (from 0.377 to 1.13 GHz) [10]. However, the antenna only covers a single frequency band. An implantable conformal antenna with wideband is presented, which uses Custave model from the CST Voxel family to simulate the SAR of 913 W/kg [11]. Although the antenna is exposed to the human body to acquire broadband characteristics, it also leads to high SAR. A symmetrical dual-loop antenna with ultrawideband ranging from 1.11 GHz to 6.06 GHz

Received 26 July 2021, Accepted 17 August 2021, Scheduled 26 August 2021
* Corresponding author: Bingwen He (1670871148@stu.xupt.edu.cn).
[1] School of Communication and Information Engineering, Xi'an University of Posts & Telecommunications, Xi'an 710100, China.
[2] China Academy of Telecommunications Research of Ministry of Industry and Information Technology, Beijing 100191, China.

is proposed to reduce the antenna loss in human body [12]. Most of these antennas use phantom human model as real environment to evaluate SAR, without considering the SAR measurement. In addition, compared with the above antennas, the loop antenna with the parasitic element is easier to achieve multi-bands and broadband.

This paper proposes a multi-band cylindrical conformal antenna for a WMCE system covering MedRadio, ISM, and WMTS bands. The parasitic opened-loop element is equivalent to the LC load, which can introduce an additional resonance 403 MHz, expand the bandwidth, and reduce the SAR values. The peak 1 g SAR values of the antenna are 83, 82, 94, and 153 W/kg at 403 MHz, 611 MHz, 915 MHz, and 2.4 GHz in the tissue-simulating liquid, and the input power below 10.4 MW satisfies human safety standards.

The proposed antenna can achieve safety diagnosis. Section 2 presents the design method and the working principle of the proposed antenna. The performance of the antenna is given in Section 3. The measurement results and discussion are presented in Section 4. The conclusion is stated in Section 5.

2. ANTENNA DESIGN

Figure 1 shows the physical layout of the multi-band cylindrical conformal antenna. The proposed antenna employs a symmetrical meanderline structure with a center loaded parasitic opened-loop element. The meanderline of the antenna increases the electrical length and minimizes the size of the antenna [13]. The proposed antenna is printed on a flat 0.2 mm-thick Rogers 5880 flexible substrate ($\varepsilon = 3.5$ and $\sigma = 0.008$ S/m). The dimension of the planar antenna is 13 mm × 27 mm × 0.017 mm. The detailed parameters are shown in Table 1 after optimization. The proposed antenna is placed into the

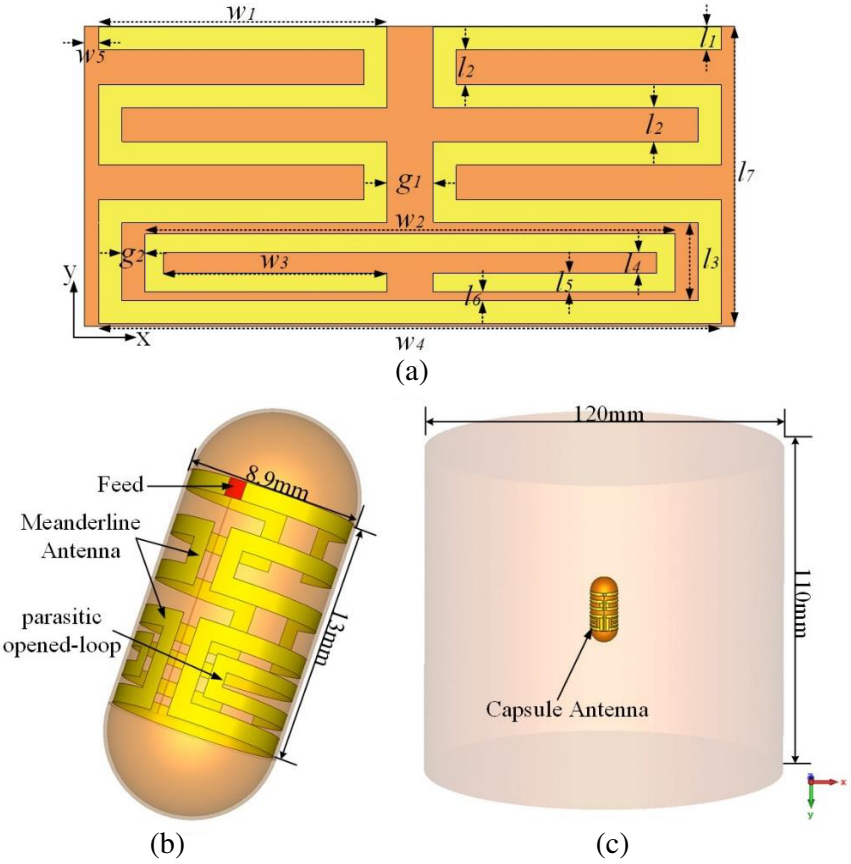

Figure 1. View of the proposed capsule antenna: (a) dimension of antenna is marked; (b) the antenna is wrapped on a capsule; (c) simulation environment in CST Microwave Studio 2020.

Table 1. Dimensions of antenna.

Parameters	Value (mm)	Parameter	Value (mm)
$w1$	12.5	$l3$	3.4
$w2$	23	$l4$	0.9
$w3$	27	$l5$	0.8
$w4$	12.5	$l6$	1.65
$w5$	0.5	$l7$	$l3$
$l1$	1	$g1$	2
$l2$	1.5	$g2$	1

inner wall of a capsule, as shown in Figure 1(b). The capsule possesses a minimum radius of 4.45 mm and a total length of 13 mm, and the thickness of shell is 0.5 mm. The capsule is made of biocompatible poly-ether-ether-ketone (PEEK, $\varepsilon = 3.2$ and $\tan\delta = 0.01$) and fabricated by 3D printing technology. The inside of the capsule is hollow, which integrates the other components of the WMCE. The proposed antenna placed in the center of uniform muscle simulation model is simulated in CST Microwave Studio 2017, as shown in Figure 1(c). The muscle model with a size of 120 mm × 110 mm (diameter × height) is selected as simulated environment, and the dielectric properties of muscle tissue are $\varepsilon_r = 56.28$ and $\sigma = 0.8$ S/m [14, 15].

The proposed antenna is optimized in a three-step design method, called Ant1, Ant2, and Ant3. Figure 2 presents the plane structure of three antennas. Three antennas are bent into cylindrical conformal shape and embedded into the same environment as that of the proposed antenna for analysis and comparison. Ant1 is designed with a simple meander loop structure. Ant2 has the same slots along the negative direction of the y-axis. The proposed antenna loads the parasitic opened-loop via enlarging gap width of the bottom slot of Ant2. Figure 3 compares the simulation results of these antennas. Ant1 generates two resonant frequencies around 900 MHz and 2.3 GHz, according to the theory of loop antenna that the circumference of loop antenna is equal to a full-wavelength. Ant2 engraves additional slots to extend the electrical length, which excites a lower resonant frequency near 700 MHz. The optimization of the slot width in y-axis can broaden the high frequency bandwidth. The parasitic opened-loop is introduced into the bottom slot of the antenna, which excites a resonance around 403 MHz. The optimized antenna covers from 0.35 GHz to 1.76 GHz (403, 433, 611, and 915 MHz) and 2.01 GHz to 3 GHz (2.4 GHz).

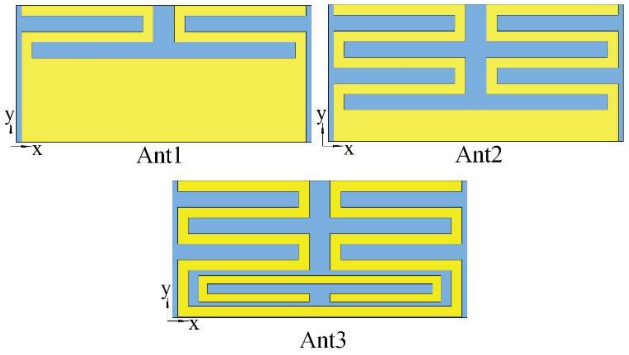

Figure 2. The planar layout of three optimized antennas.

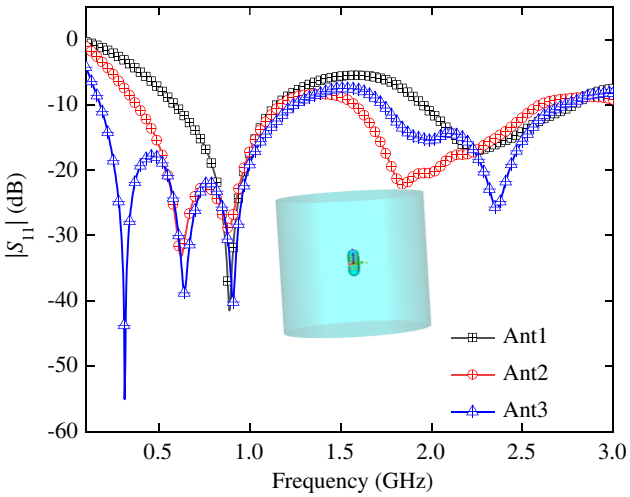

Figure 3. Simulated $|S_{11}|$ of three antennas.

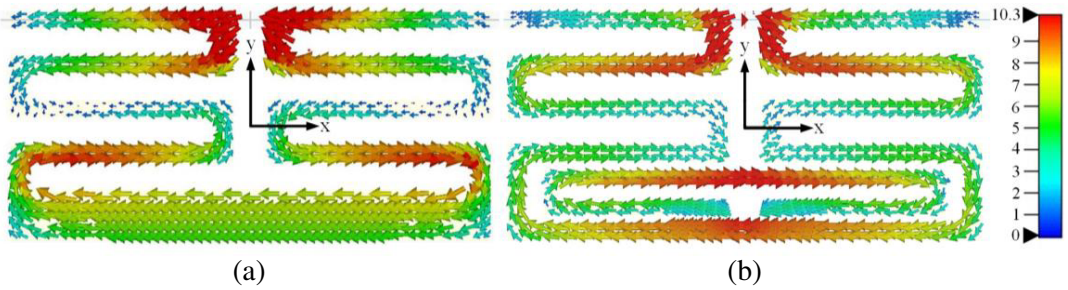

Figure 4. Current distribution of the loop antenna at 403 MHz: (a) without the parasitic opened-loop element; (b) with the parasitic opened-loop element.

Figure 4 compares the current distributions of the proposed planar antenna with and without a parasitic opened-loop structure to evaluate the working principle of the proposed antenna. The current concentrates on the above edge of the bottom slot when the antenna operates at 403 MHz in Figure 4(a). The current path does not reach the resonant point length required by 403 MHz and 433 MHz, according to the loop antenna theory. As can be seen from Figure 5, no resonant frequency is generated at 403 MHz as the proposed antenna has no parasitic element. The current of the lower edge of the bottom slot contributes little to radiation. The fundamental frequency resonance at 403 MHz is generated by loading the parasitic element to gather the strong current at the lower edge of the bottom slot and extend the current path in Figure 4(b). The parasitic element can be equivalent to an LC resonant circuit, which excites a new lower resonance and reduces loop inductance to improve the impedance matching of the antenna.

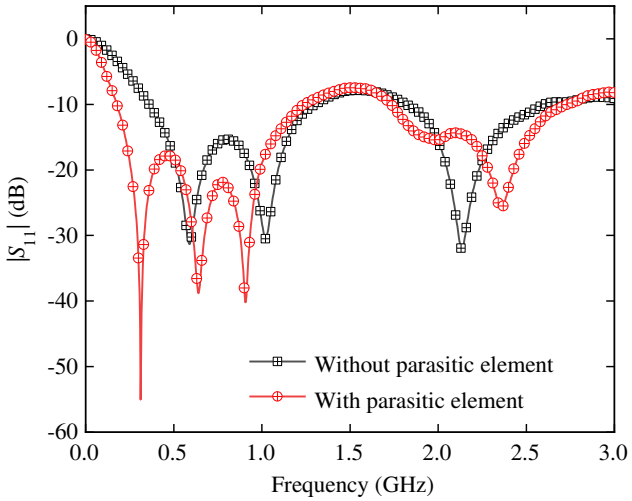

Figure 5. The $|S_{11}|$ of antenna with and without the parasitic opened-loop element.

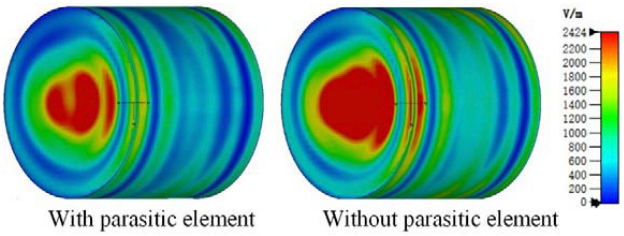

Figure 6. The E-field distribution around the proposed antenna with and without the parasitic in the simplified muscle phantom at 403 MHz.

Figure 6 presents the scalar electric near field (E-field) across the center of the antenna with and without the parasitic element in uniform muscle simulation model. The inner loop reduces the power absorption to degrade the SAR by reducing the near electric field of the antenna.

3. ANTENNA PERFORMANCE

3.1. Environment and System Consideration

The proposed antenna is ingested into the human model Glenn in the FDTD-based simulator for simulating the effect of the complex electromagnetic tissues around the GI tract on the antenna. The dielectric properties of each part of the tissue are listed in Table 2. The characteristics of the antenna in colon, muscle, small intestine, and stomach are simulated for analyzing the impedance performance of the antenna. The antenna characteristics are only disturbed by the neighboring tissues, thus using the human model Glenn, as shown in Figure 7. The model has more than 300 tissues and organs, and accuracy with a resolution of $0.5 \times 0.5 \times 0.5\,\text{mm}^2$ throughout the entire body. The $|S_{11}|$ of the proposed antenna in the colon, muscle, small intestine, and stomach of the Glenn present wideband characteristics, as shown in Figure 8(a). The antenna has a narrow impedance bandwidth at lower frequency band, ranging from 213 to 1243 MHz due to the largest relative dielectric constant in the stomach among all parts of the tissue. The impedance bandwidth still covers the low frequency bands of requirement, even though the impedance bandwidth of the antenna in each part of the tissue is different. Result indicates that our proposed antenna has strong anti-interference in various tissues.

Table 2. Properties and SAR value of various parts of gastrointestinal tract [16].

Organization scenario	Stomach	Colon	Small Intestine	Muscle
ε	67.3	62.1	65.5	56.8
σ (S/m)	1.03	0.85	1.95	0.82

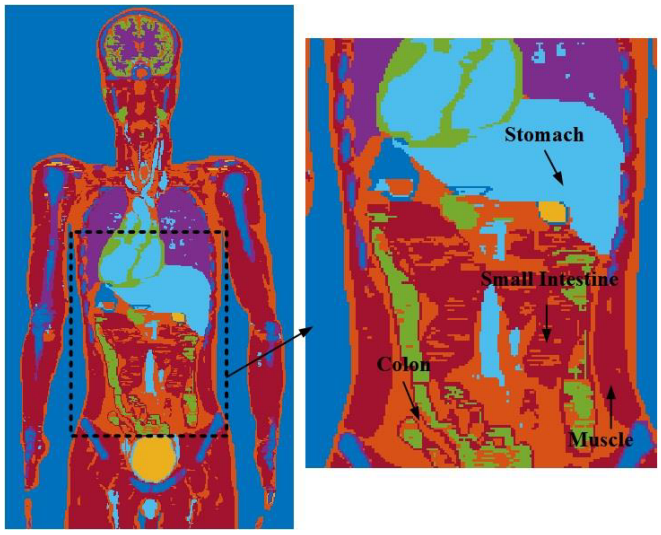

Figure 7. Glenn voxel model and the implantation site of antenna.

The conductive elements in the capsule system will deteriorate the proposed antenna performance. Therefore, a perfect conductor cylinder with diameter of 7 mm and height of 4 mm as the battery model is placed at the bottom of the capsule, as shown in the attached figure in Figure 8(b). The three situations of no battery, the bottom of the antenna facing to the battery, and the upper of the antenna facing the battery are simulated, respectively. The results show that the disturbance of the radiation field around the conductive elements to the antenna at different positions is negligible, and the impedance matching of the antenna is stable.

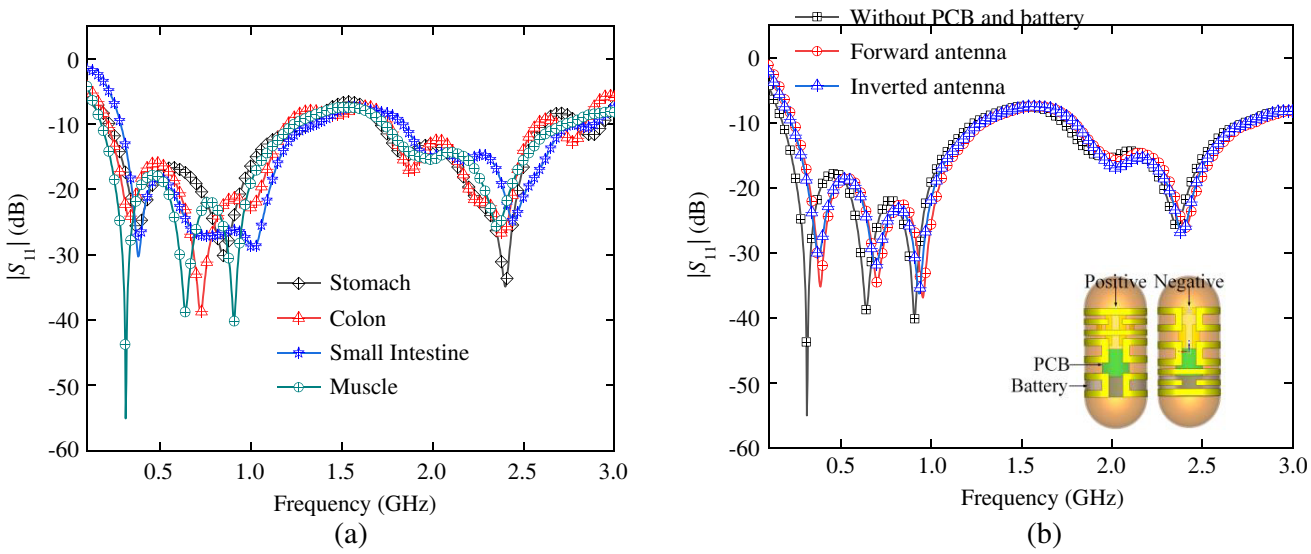

Figure 8. $|S_{11}|$ of the capsule antenna in different environments are simulated for robust analysis: (a) The antennas are in the tissues of GI; (b) The position of the antenna relative to the electronic component.

3.2. Safety of Antenna

The SAR analysis is implemented in the human model Glenn. In small intestine, the SAR values of muscle-simulating are 112, 131, 159, and 213 W/kg at 0.403, 0.433, 0.915, and 2.4 GHz when the antenna input power is set at 1 W. The SAR values of the antenna are diverse in different tissues due to the variable conductivity. Therefore, the SAR value of 1 g in small intestine is the largest among the four parts. The maximum permissible input powers of the antenna are 14.28, 12.21, 10.06, 7.51 mW, according to IEEE C95.1-1999 standard rules that SAR per 1 g of tissue should not exceed 1.6 W/kg. Table 3 shows the SAR simulated results of the antenna in various parts of GI. These results are far above the licensed effective isotropic radiated power -40 dBm (100 μW) of ETSIEN 303 520 V1.2.1 standard, which indicate that the antenna meets human safety specifications and can be used for medical diagnosis.

Table 3. SAR value of various parts of gastrointestinal tract.

Organization scenario	Stomach	Colon	Small Intestine	Muscle
Frequency (GHz)	1-g SAR (W/kg)			
0.403	98	89	112	81
0.433	103	97	131	83
0.915	115	108	159	95
2.4	198	183	213	149

4. RESULT AND DISCUSSION

Figure 9(a) presents that the plane antenna is wrapped on the surface of the 3D printed capsule shell which is 0.5 mm thick. Then, a layer of biocompatible polyimide is coated on the antenna surface for preventing direct contact between radiators and pork. The antenna is welded to a 10 cm long 50 Ω RF line and connected to a calibrated Agilent N5244A Vector Network Analyzer (VNA) port. It is put into a 150 mm × 100 mm × 50 mm cuboid pork block as the measuring environment, and the $|S_{11}|$ is

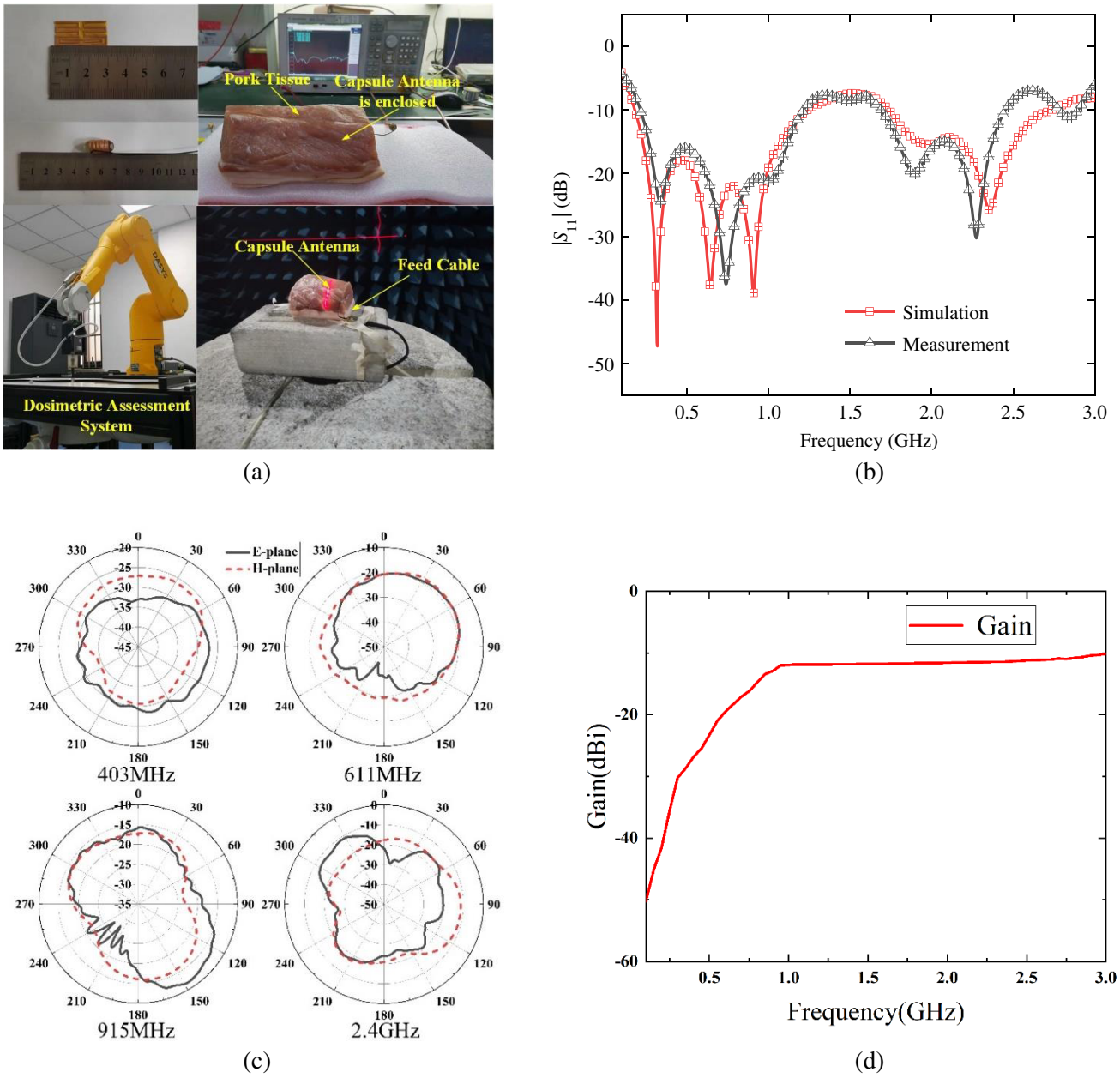

Figure 9. Antenna measurement results: (a) fabricated antenna and measurement environment; (b) comparison of the real measurement and the simulation for $|S_{11}|$; (c) measured radiation patterns at 403, 611, 915, 2400 MHz and (d) the gain curve in the frequency band.

presented. Figure 9(b) presents the measured relative bandwidth which reaches 133% in ISM, MedRadio and MICS bands, having slight deviation from the simulation result. The deviation of the bandwidth and frequency shift (FS) may be caused by the welded feeder error. Another reason is that the dielectric properties of the fat and lean proportions in the pork are different from that of the uniform muscle in the simulation.

The radiation patterns of the proposed antenna are measured in a SATIMO 64 probe anechoic chamber, as shown in Figure 9(a). Figure 9(c) displays measured different patterns in H and E planes at 403 MHz, 611 MHz, 915 MHz, 2.4 GHz, and Figure 9(d) shows the gain curve in the interested frequency band. The maximum far-field gains of the capsule antenna embedded in the pork are

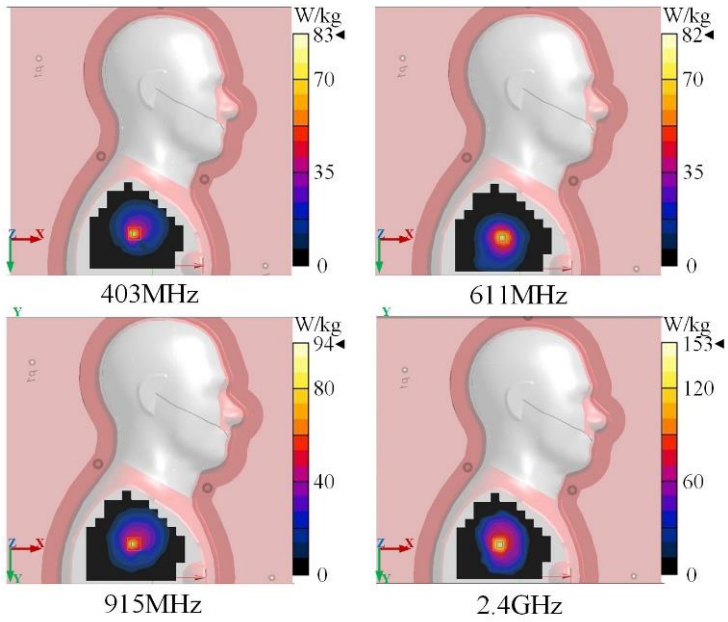

Figure 10. The SAR distributions over 1-g of tissue in the tissue-simulating liquid at 403, 611, 915, 2400 MHz.

−26.6 dBi, −18.9 dBi, −11.8 dBi, −11.6 dBi, and radiation efficiencies are 0.45%, 1.2%, 4.3%, 5.9% for the (403, 611, 915, 2400) MHz designs, respectively. The H and E planes of the antenna have the omnidirectional radiation characteristic which can maintain a stable wireless link of WMCE for withstanding the unknown orientation of capsule in GI.

Figure 9(a) shows that the Dosimetric Assessment System 6 (DASY6) measures the averaged SAR distributions in tissue-simulating liquid. Dielectric properties of the liquid are the same as the simulated muscle tissue. The liquid is formed with DGBE, Triton X-100, de-ionized water, agarose. The antenna is placed on the chest of the model to measure the SAR distributions, as shown in Figure 10. The figure shows that the 1-g peak SAR values are 83, 82, 94, 153 W/kg with the maximum allowable powers of the proposed antenna are 19.2, 19.5, 17.0, 10.4 mW at 403 MHz, 611 MHz, 915 MHz, 2.4 GHz, respectively. The antenna cannot provide power for every operating band since it has only one input port. Hence,

Table 4. Comparison of the proposed antenna with prior work: antenna type, bandwidth, gain, SAR.

Ref.	Antenna type	Frequency (MHz)	Bandwidth (GHz)	Max Gain (dBi)	1-g SAR (W/kg) (Small Intestine)
[7]	Conformal IFA	402, 915, 2400	50, 103, 435	−29.7, −24.9, −23.2	216.6, 92.4, 98.5
[10]	Conformal structure	433	0.337–1.13	−19.8	354.5
[11]	Conformal structure	403	0.284–0.825	−31.5	913
[12]	Conformal Loop	2400	1.11–6.03	−12.6	215.7
Our antenna	Conformal Loop	403, 611, 915, 2400	0.35–1.76, 1.95–3	−26.6, −18.9, −11.8, −11.3	83, 82, 94, 153

the result is safe for human body when the input power is below 10.4 mW. The SAR values confirm that the proposed antenna completely complies with human safety standards.

Table 4 shows that the proposed antenna is compared with the previous capsule antennas to demonstrate the advantage of the proposed antenna. The table compares different operating frequency, impedance matching bandwidth, 1-g SAR values in the reported phantom. The results indicate that our antenna owns better performance than the previous capsule antennas for multiband operation, SAR, and impedance bandwidth. The antenna is a promising candidate for WMCE systems.

5. CONCLUSION

A multi-band cylindrical conformal capsule antenna operates at 915 MHz and 2.4 GHz ISM bands, 403 MHz MedRadio band, and 611 MHz WMTS is proposed. The parasitic opened-loop element has two characteristics, which elongates current path at low-frequency to generate 403 MHz while the impedance matching is improved and reduces the SAR values of the antenna by reducing the near electric field. The test results show that the bandwidths at four bands of measurements include 0.35 GHz–1.761 GHz and 1.95 GHz–3 GHz. The peak gains and the peak 1 g SAR values at 403 MHz, 611 MHz, 915 MHz, 2.4 GHz are −26.6 dBi, −18.9 dBi, −11.8 dBi, −11.3 dBi, and 83, 82, 94, 153 W/kg, respectively. Results indicate that the proposed antenna is a good candidate for multi-band capsule endoscope.

ACKNOWLEDGMENT

This work was supported by the Shaanxi Provincial Key Research and Development Program of China under Grant 2018ZDCXL-GY-04-01.

REFERENCES

1. Kissi, C., M. Särestöniemi, T. Kumpuniemi, S. Myllymäki, M. Sonkki, J.-P. Mäkelä, M. N. Srifi, H. Jantunen, and C. Pomalaza-Raez, "Receiving UWB antenna for wireless capsule endoscopy communications," *Progress In Electromagnetics Research C*, Vol. 101, 53–69, 2020.
2. Xing, B., Y. Zhang, H. Zou, and Z. Liu, "A conformal quasi-isotropic dielectric resonator antenna for wireless capsule endoscope application," *Progress In Electromagnetics Research M*, Vol. 99, 211–221, 2021.
3. Patil, K. S. and E. Rufus, "A review on antennas for biomedical implants used for IoT based health care," *Sensor Review*, Vol. 40, 273–280, 2019.
4. Peng, Y., K. Saito, and K. Ito, "Antenna design for impulse-radio-based wireless capsule endoscope communication systems," *IEEE Transactions on Antennas and Propagation*, Vol. 66, 5031–5042, 2018.
5. Duan, Z., L.-J. Xu, S. Gao, and G. Wen, "Integrated design of wideband omnidirectional antenna and electronic components for wireless capsule endoscopy systems," *IEEE Access*, Vol. 6, 29626–29636, 2018.
6. Fiedler, T. M., M. E. Ladd, and A. K. Bitz, "SAR simulations & safety," *Neuroimage*, Vol. 168, 33–58, 2018.
7. Bao, Z., Y. Guo, and R. Mittra, "Single-layer dual-/tri-band inverted-F antennas for conformal capsule type of applications," *IEEE Transactions on Antennas and Propagation*, Vol. 65, 7257–7265, 2017.
8. Das, R. and H. Yoo, "A multiband antenna associating wireless monitoring and nonleaky wireless power transfer system for biomedical implants," *IEEE Transactions on Microwave Theory and Techniques*, Vol. 65, 2485–2495, 2017.
9. Yousaf, M., I. B. Mabrouk, F. Faisal, M. Zada, Z. Bashir, A. Akram, and H. Yoo, "Compacted conformal implantable antenna with multitasking capabilities for ingestible capsule endoscope," *IEEE Access*, Vol. 8, 157617–157627, 2020.

10. Shang, J. and Y. Yu, "An ultrawideband and conformal antenna for wireless capsule endoscopy," *Microwave and Optical Technology Letters*, Vol. 62, 860–865, 2020.
11. Wang, J., M. Leach, E. G. Lim, Z. Wang, R. Pei, and Y. Huang, "An implantable and conformal antenna for wireless capsule endoscopy," *IEEE Antennas and Wireless Propagation Letters*, Vol. 17, 1153–1157, 2018.
12. Shang, J. and Y. Yu, "An ultrawideband capsule antenna for biomedical applications," *IEEE Antennas and Wireless Propagation Letters*, Vol. 18, 2548–2551, 2019.
13. Basir, A., M. Zada, Y. Cho, and H. Yoo, "A dual-circular-polarized endoscopic antenna with wideband characteristics and wireless biotelemetric link characterization," *IEEE Transactions on Antennas and Propagation*, Vol. 68, 6953–6963, 2020.
14. Gabriel, S., R. W. Lau, and C. Gabriel, "The dielectric properties of biological tissues: III. Parametric models for the dielectric spectrum of tissues," *Physics in Medicine and Biology*, Vol. 41, 2271–2293, 1996.
15. Gabriel, S., R. W. Lau, and C. Gabriel, "The dielectric properties of biological tissues: II. Measurements in the frequency range 10 Hz to 20 GHz," *Physics in Medicine and Biology*, Vol. 41, 2251–2269, 1996.
16. Ga Briel, C. and A. Peyman, "Dielectric properties of biological tissues; Variation with age — Science direct," *Conn's Handbook of Models for Human Aging (Second Edition)*, 939–952, 2018.